

# Dressed intensity noise correlation and intensity-difference squeezing of spontaneous parametric four-wave mixing process in a $\text{Pr}^{3+}$ :YSO crystal

Irfan Ahmed,<sup>1,2</sup> Zheng Liu,<sup>1</sup> Yan Pan,<sup>1</sup> Changbiao Li,<sup>1</sup> Imran Ali Metlo,<sup>1</sup> Haixia Chen,<sup>1</sup> Ruimin Wang,<sup>1,3</sup> and Yanpeng Zhang,<sup>1,4</sup>

<sup>1</sup>Key Laboratory for Physical Electronics and Devices of the Ministry of Education & Shaanxi Key Lab of Information Photonic Technique, Xi'an Jiaotong University, Xi'an 710049, China

<sup>2</sup>Department of Electrical Engineering, Sukkur IBA, Sukkur 65200, Sindh, Pakistan

<sup>3</sup>wangrm@mail.xjtu.edu.cn

<sup>4</sup>ypzhang@mail.xjtu.edu.cn

**Abstract:** We report dressed intensity noise correlation and intensity-difference squeezing based on spontaneous parametric four-wave mixing (SP-FWM) in  $\text{Pr}^{3+}$ : $\text{Y}_2\text{SiO}_5$  crystal both experimentally and theoretically. We found such intensity noise correlation and intensity-difference squeezing can be controlled by using the dressing effect to manipulate the nonlinear optical coefficient of the SP-FWM process. By changing detuning and power of the optical field, we manipulate the nonlinear optical coefficient of the SP-FWM process, thus control the correlation and squeezing. The results show stronger correlation and squeezing with single dressing, while weaker near the resonant point due to destructive double dressing. Furthermore, we observed the dependence of correlation times on the power of dressing field, and explained by the combination of the dressing effect and induced dipole-dipole interaction. We also showed the fourth-order fluorescence signals accompanying with the SP-FWM process.

©2015 Optical Society of America

**OCIS codes:** (190.4380) Nonlinear optics, four-wave mixing; (190.4180) Multiphoton processes; (300.2570) Four-wave mixing; (270.1670) Coherent optical effects.

---

## References and links

1. H. Wang, D. Du, Y. Fan, A. Li, L. Wang, X. Wei, Z. Kang, Y. Jiang, J. Wu, and J. Gao, "Enhanced four-wave mixing by atomic coherence in  $\text{Pr}^{3+}$ : $\text{Y}_2\text{SiO}_5$  crystal," *Appl. Phys. Lett.* **93**(23), 231107 (2008).
2. H. Wang, Z. Kang, Y. Jiang, Y. Li, D. Du, X. Wei, J. Wu, and J. Gao, "Erasure of stored optical information in a  $\text{Pr}^{3+}$ : $\text{Y}_2\text{SiO}_5$  crystal," *Appl. Phys. Lett.* **92**(1), 011105 (2008).
3. Y. Zhao, C. Wu, B. Ham, M. Kim, and E. Awad, "Microwave induced transparency in Ruby," *Phys. Rev. Lett.* **79**(4), 641–644 (1997).
4. C. Wei and N. Manson, "Observation of electromagnetically induced transparency within an electron spin resonance transition," *J. Opt. B* **1**(4), 464–468 (1999).
5. B. Ham, P. Hemmer, and M. Shahriar, "Efficient electromagnetically induced transparency in a rare-earth doped crystal," *Opt. Commun.* **144**(4-6), 227–230 (1997).
6. M. C. Phillips, H. Wang, I. Rumyantsev, N. H. Kwong, R. Takayama, and R. Binder, "Electromagnetically induced transparency in semiconductors via Biexciton coherence," *Phys. Rev. Lett.* **91**(18), 183602 (2003).
7. Y. Du, Y. Zhang, C. Zuo, C. Li, Z. Nie, H. Zheng, M. Shi, R. Wang, J. Song, K. Lu, and M. Xiao, "Controlling four-wave mixing and six-wave mixing in a multi-Zeeman-sublevel atomic system with electromagnetically induced transparency," *Phys. Rev. A* **79**(6), 063839 (2009).
8. M. Sabooni, Q. Li, L. Rippe, R. K. Mohan, and S. Kröll, "Spectral engineering of slow light, cavity line narrowing, and pulse compression," *Phys. Rev. Lett.* **111**(18), 183602 (2013).
9. A. V. Turukhin, V. S. Sudarshanam, M. S. Shahriar, J. A. Musser, B. S. Ham, and P. R. Hemmer, "Observation of ultraslow and stored light pulses in a solid," *Phys. Rev. Lett.* **88**(2), 023602 (2001).

10. J. J. Longdell, E. Fraval, M. J. Sellars, and N. B. Manson, "Stopped light with storage times greater than one second using electromagnetically induced transparency in a solid," *Phys. Rev. Lett.* **95**(6), 063601 (2005).
11. F. Beil, J. Klein, G. Nikoghosyan, and T. Halfmann, "Electromagnetically induced transparency and retrieval of light pulses in a  $\Lambda$ -type and a V-type level scheme in  $\text{Pr}^{3+}:\text{Y}_2\text{SiO}_5$ ," *J. Phys. B* **41**(7), 074001 (2008).
12. C. Li, L. Wang, H. Zheng, H. Lan, C. Lei, D. Zhang, M. Xiao, and Y. Zhang, "All-optically controlled fourth- and sixth-order fluorescence processes of  $\text{Pr}^{3+}:\text{YSO}$ ," *Appl. Phys. Lett.* **104**(5), 051912 (2014).
13. Z. Y. Ou, S. F. Pereira, H. J. Kimble, and K. C. Peng, "Realization of the Einstein-Podolsky-Rosen paradox for continuous variables," *Phys. Rev. Lett.* **68**(25), 3663–3666 (1992).
14. A. Heidmann, R. J. Horowicz, S. Reynaud, E. Giacobino, C. Fabre, and G. Camy, "Observation of quantum noise reduction on twin laser beams," *Phys. Rev. Lett.* **59**(22), 2555–2557 (1987).
15. A. S. Coelho, F. A. Barbosa, K. N. Cassemiro, A. S. Villar, M. Martinelli, and P. Nussenzveig, "Three-color entanglement," *Science* **326**, 823 (2009).
16. H. Chen, M. Qin, Y. Zhang, X. Zhang, F. Wen, J. Wen, and Y. Zhang, "Parametric amplification of dressed multi-wave mixing in atomic ensemble," *Laser Phys. Lett.* **11**(4), 045201 (2014).
17. Y. Zhang, A. W. Brown, and M. Xiao, "Opening four-wave mixing and six-wave mixing channels via dual electromagnetically induced transparency windows," *Phys. Rev. Lett.* **99**(12), 123603 (2007).
18. Y. Zhang, U. Khadka, B. Anderson, and M. Xiao, "Temporal and spatial interference between four-wave mixing and six-wave mixing channels," *Phys. Rev. Lett.* **102**(1), 013601 (2009).
19. B. Wu and M. Xiao, "Bright correlated twin beams from an atomic ensemble in the optical cavity," *Phys. Rev. A* **80**(6), 063415 (2009).
20. V. Boyer, A. M. Marino, R. C. Pooser, and P. D. Lett, "Entangled images from four-wave mixing," *Science* **321**(5888), 544–547 (2008).
21. Z. Nie, H. Zheng, P. Li, Y. Yang, Y. Zhang, and M. Xiao, "Interacting multi wave mixing in a five-level atomic system," *Phys. Rev. A* **77**(6), 063829 (2008).
22. M. Fleischhauer, A. Imamoglu, and J. P. Marangos, "Electromagnetically induced transparency: Optics in coherent media," *Rev. Mod. Phys.* **77**(2), 633–673 (2005).

## 1. Introduction

Quantum correlation plays vital role for motivational research for possible applications of quantum communication and quantum information processing. The generations of correlated and entangled photon pairs by parametric processes have been widely studied, including parametric down-conversion process in nonlinear crystals [1, 2]. Correlated beams have also been generated by using an optical parametric amplification process in atomic media [3]. Besides these, the correlation switching in an atomic system has been experimentally demonstrated [4]. The amplitude and intensity noise correlations of counter-propagating paired photons in an atomic system have also been discussed theoretically [5]. Simultaneously, the great deal of work has been done in developing the control mechanism for nonlinear optical process, such as influence of a dressing field on parametric amplification of multi-wave mixing processes in an atomic system [6], polarization dressed multi-order fluorescence [7], interaction of double dressed multi-waves mixing in five level atomic systems [8]. Currently, the most experimental studies of the parametric FWM processes based on atomic coherence have been carried out in atomic gases. However, for many practical applications, the corresponding researches in solid materials are more valuable. The rare-earth-ion-doped crystals  $\text{Pr}^{3+}:\text{Y}_2\text{SiO}_5$  ( $\text{Pr}^{3+}:\text{YSO}$ ) in which the atomic coherence can be induced easily when interacting with multiple laser fields, have been used to realize electromagnetically induced transparency (EIT) [9–12], coherent storage and light velocity reduction [13–15], enhanced FWM process and all-optically controlled higher-order fluorescence signal with and without splitting [16].

In this paper, we use the SP-FWM process in  $\text{Pr}^{3+}:\text{Y}_2\text{SiO}_5$  crystal to generate the intensity noise correlation and intensity-difference squeezing and investigate the control mechanism of the noise correlation and intensity-difference squeezing. The V-type and  $\Lambda$ -type three-level systems of  $\text{Pr}^{3+}:\text{YSO}$  are compared. We showed that the correlation and squeezing may be manipulated by the detuning and power of the optical field participating in the SP-FWM process. But there is some difference between V-type and  $\Lambda$ -type three-level systems due to difference of dipole-dipole interaction and dressing effect. We also showed the fourth-order fluorescence signals accompanying with the SP-FWM process. Finally, the correlation time of SP-FWM is also investigated by changing power. The paper is constructed as following: in Sec.

2, we show the experimental setup for the generation of intensity noise correlation and intensity-difference squeezing in  $\text{Pr}^{3+}$ : YSO crystal and introduce the corresponding theory briefly; in Sec. 3, we present the experiment results and discuss them in detail; in Sec. 4, we conclude the paper.

## 2. Basic theory and experimental scheme

### 2.1 Experimental setup

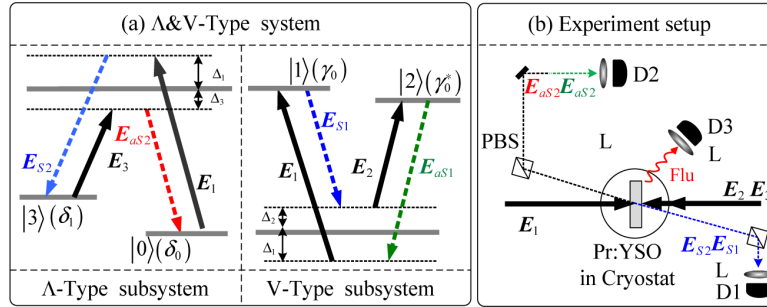


Fig. 1. (a) Two three-level subsystems ( $\Lambda$ -type and V-type) in  $\text{Pr}^{3+}$ :YSO crystal and the laser coupling configuration. (b) Experimental setup scheme.  $\Delta_i$ : frequency detuning of ( $\mathbf{E}$ ), field, FL: fluorescence, D: photomultiplier tube, PBS: polarized beam splitter, BS: beam splitter, and L: lens

The sample used in this experiment is 0.05% rare-earth  $\text{Pr}^{3+}$  doped  $\text{Y}_2\text{SiO}_5$  crystal, the triplet energy-level  $^3\text{H}_4$  and singlet energy-level  $^1\text{D}_2$  of  $\text{Pr}^{3+}$  ions are selected. The degeneracy of the energy levels of the  $\text{Pr}^{3+}$  ion is removed by the crystal field of YSO, where the terms in  $^3\text{H}_4$  and  $^1\text{D}_2$  states are split into nine and five Stark components, respectively. The  $\text{Pr}^{3+}$  ions occupy two nonequivalent cation sites (sites I and II, respectively) in the YSO crystal lattice. The energy levels are labeled by a Greek letter with and without asterisk for site II and I sites, respectively. The coupling between  $\text{Pr}^{3+}$  ions localized at different cation vacancies can happen due to dipole-dipole interactions, so one can treat the two ions as a heteronuclear-like molecule. Therefore, we can construct a V-type three-level subsystem ( $|0\rangle(\delta_0) \leftrightarrow |1\rangle(\gamma_0) \leftrightarrow |2\rangle(\gamma_0^*)$ ) and a  $\Lambda$ -type ( $|0\rangle(\delta_0) \leftrightarrow |1\rangle(\gamma_0) \leftrightarrow |3\rangle(\delta_1)$ ) by coupling the corresponding laser fields as shown in Fig. 1(a).

The sample (a 3-mm Pr:YSO crystal) is held at 77 K in a cryostat (CFM-102). Three tunable dye lasers (narrow scan with a  $0.04 \text{ cm}^{-1}$  line width) pumped by an injection locked single-mode Nd:YAG laser (Continuum Powerlite DLS 9010, 10 Hz repetition rate, 5 ns pulse width) are used to generate the pumping fields  $\mathbf{E}_1$  ( $\omega_1, \Delta_1$ ),  $\mathbf{E}_2$  ( $\omega_2, \Delta_2$ ), and  $\mathbf{E}_3$  ( $\omega_3, \Delta_3$ ). Their frequency detuning is defined as  $\Delta_i = \omega_{mn} - \omega_i$  ( $i = 1, 2, \text{ and } 3$ ), where  $\omega_{mn}$  denotes the corresponding atomic transition frequency and  $\omega_i$  is the laser frequency. In the V-type (or  $\Lambda$ -type) three-level subsystem, a SP-FWM processes satisfying the phase-matching condition  $\mathbf{k}_1 + \mathbf{k}_2 = \mathbf{k}_{S1} + \mathbf{k}_{aS1}$  (or  $\mathbf{k}_1 + \mathbf{k}_3 = \mathbf{k}_{S2} + \mathbf{k}_{aS2}$ ) can occur, where  $\mathbf{k}_{S1}$  and  $\mathbf{k}_{aS1}$  ( $\mathbf{k}_{S2}$  and  $\mathbf{k}_{aS2}$ ) are the wavevectors of the generated Stokes and anti-Stokes fields in the V-type system ( $\Lambda$ -type system), respectively. Since the SP-FWM process absorbs two photons and produces one Stokes and one anti-Stokes photon simultaneously, the two output photons of the SP-FWM process are highly correlated. Figure 1(b) shows the experimental arrangement. The generated Stokes signal  $\mathbf{E}_{S1}$  (or  $\mathbf{E}_{S2}$ ) and anti-Stokes signal  $\mathbf{E}_{aS1}$  (or  $\mathbf{E}_{aS2}$ ) are reflected by polarized beam splitters (PBS) and detected by photomultiplier tubes. The intensity noises correlation between Stokes and anti-Stokes signals can be calculated by using their time-dependent intensity fluctuations, which are recorded by D1 and D2 and denoted as  $\delta \hat{I}_S(t_S)$  and  $\delta \hat{I}_{aS}(t_{aS})$ . The fluorescence signals accompanying with the SP-FWM process is simultaneously detected by D3.

## 2.2 Basic theory

### 2.2.1 Density matrix elements and nonlinear coefficient

Now we present a brief theory for the generated correlation from the SP-FWM process both in V-type and  $\Lambda$ -type systems. Signals  $\mathbf{E}_{aS}$  and  $\mathbf{E}_S$  are generated by opening  $\mathbf{E}_1$  and  $\mathbf{E}_2$  ( $\mathbf{E}_1$  and  $\mathbf{E}_3$ ) beams in the V-type ( $\Lambda$ -type) system. For the  $\Lambda$ -type system, according to the Liouville pathways [17,18], the density matrix elements  $\rho_{13(S2)}^{(3)}$  for Stokes signal  $\mathbf{E}_{S2}$  can be obtained as:

$$\rho_{13(S2)}^{(3)} = -iG_3 G_{aS2}^* G_1 / [(\Gamma_{13} + i\Delta_3)(\Gamma_{13} + i\Delta_1)\Gamma_{30}] \quad \text{via perturbation chain}$$

$$\rho_{33}^{(0)} \xrightarrow{E_3} \rho_{13}^{(1)} \xrightarrow{E_{aS2}^*} \rho_{03}^{(2)} \xrightarrow{E_3} \rho_{13(S2)}^{(3)}, \quad \text{and } \rho_{10(aS2)}^{(3)} \text{ for anti-Stokes signal } \mathbf{E}_{aS2} \text{ can be}$$

$$\text{obtained as: } \rho_{10(aS2)}^{(3)} = -iG_1 G_{2S2}^* G_3 / [(\Gamma_{10} + i\Delta_1)(\Gamma_{10} + i\Delta_3)\Gamma_{30}] \quad \text{via}$$

$$\rho_{00}^{(0)} \xrightarrow{E_1} \rho_{10}^{(1)} \xrightarrow{E_{aS2}^*} \rho_{30}^{(2)} \xrightarrow{E_3} \rho_{10(aS2)}^{(3)}. \quad \text{Here, } G_i = \mu E_i / \hbar \text{ is the Rabi frequency of the } \mathbf{E}_i$$

field, the term  $\Gamma_{ij}$  is the decay rate between the energy levels  $|i\rangle$  and  $|j\rangle$ . If the powers of  $\mathbf{E}_1$  and  $\mathbf{E}_3$  fields are strong enough, we should consider dressing effect from  $\mathbf{E}_1$  and  $\mathbf{E}_3$  fields. Then the density matrix elements with double dressing effect should be modified as:

$$\rho_{13S2}^{(3)} = \frac{-iG_3 G_{aS2}^* G_1}{(\Gamma_{13} + i\Delta_3) \left\{ \Gamma_{13} + i\Delta_1 + G_3^2 / [\Gamma_{13} + i(\Delta_1 - \Delta_3)] \right\} (\Gamma_{03} + G_1^2 / [\Gamma_{13} + i\Delta_1])} \quad (1)$$

$$\rho_{10aS2}^{(3)} = \frac{-iG_1 G_{S2}^* G_3}{(\Gamma_{10} + i\Delta_1) \left\{ \Gamma_{10} + i\Delta_3 + G_1^2 / [\Gamma_{13} - i(\Delta_1 - \Delta_3)] \right\} (\Gamma_{30} + G_3^2 / [\Gamma_{10} + i\Delta_3])} \quad (2)$$

Likewise, the density matrix elements with double dressing effect of  $\mathbf{E}_1$  and  $\mathbf{E}_2$  in V-type system can be written as

$$\rho_{10S1}^{(3)} = \frac{-iG_{aS1}^* G_1 G_2}{(\Gamma_{20} + i\Delta_2) \left\{ \Gamma_{00} + i(\Delta_2 - \Delta_1) + G_2^2 / [\Gamma_{20} + i(\Delta_2 - \Delta_1) + G_1^2 / (\Gamma_{01} - i\Delta_1)] \right\} (\Gamma_{10} + i\Delta_1 + G_1^2 / \Gamma_{11})} \quad (3)$$

$$\rho_{20aS1}^{(3)} = \frac{-iG_1 G_{S1}^* G_2}{(\Gamma_{10} + i\Delta_1) \left\{ \Gamma_{00} + i(\Delta_1 - \Delta_2) + G_2^2 / [\Gamma_{20} + G_1^2 / (\Gamma_{21} - i\Delta_1)] \right\} (\Gamma_{20} + i\Delta_2 + G_1^2 / \Gamma_{22})} \quad (4)$$

Once the Stokes and anti-Stokes signals are generated, they will propagate through the nonlinear medium. The nonlinear coefficients  $\kappa_{S/aS}$  are determined by the nonlinearity susceptibility  $\chi_{S/aS}^{(3)}$  and the amplitude of incident fields, and can be given as

$$\kappa_{S/aS} = \left| (-i\omega_{S/aS} / 2c) \chi_{S/aS}^{(3)} E_1 E_j \right| \quad (5)$$

Where  $c$  is speed of light, and  $\omega_{S/aS}$  is the angular frequency. Because of the relation of  $\chi_{S/aS}^{(3)} = N\mu\rho_{(S/aS)}^{(3)} / (\epsilon_0 E_1 E_j E_{aS/S}^*)$ , where  $j = 2$  (V-type) or  $3$  ( $\Lambda$ -type),  $N$  is atomic density,  $\mu$  is corresponding dipole moment, and  $\epsilon_0$  is permittivity of free space, the SP-FWM process can be controlled by the fields  $\mathbf{E}_1$  and  $\mathbf{E}_2$  (or  $\mathbf{E}_3$ ). Then the output photon number from the nonlinear medium can be written as

$$\hat{N}_S = \hat{a}_S^+(L)\hat{a}_S(L) = Q\hat{a}_S^+(0)\hat{a}_S(0) + (Q-1)\hat{a}_{aS}^+(0)\hat{a}_{aS}^+(0) + \sqrt{Q(Q-1)}\hat{a}_S^+(0)\hat{a}_{aS}^+(0) + \sqrt{Q(Q-1)}\hat{a}_{aS}^+(0)\hat{a}_S(0) \quad (6)$$

$$\hat{N}_{aS} = \hat{a}_{aS}^+(L)\hat{a}_{aS}(L) = Q\hat{a}_{aS}^+(0)\hat{a}_{aS}(0) + (Q-1)\hat{a}_S(0)\hat{a}_S^+(0) + \sqrt{Q(Q-1)}\hat{a}_{aS}^+(0)\hat{a}_S^+(0) + \sqrt{Q(Q-1)}\hat{a}_S(0)\hat{a}_{aS}(0) \quad (7)$$

where  $\hat{a}_i$  and  $\hat{a}_i^+$  ( $i = S$  or  $aS$ ) represent annihilation and creation operators, respectively.  $Q = \cosh^2(\kappa_{S/aS}L)$  is the gain coefficient with the medium length  $L$ .

### 2.2.2 Intensity noise correlation and intensity difference squeezing

The measured photon number at each output channel can be obtained by  $\langle \hat{a}_i^+ \hat{a}_i \rangle$  and the corresponding intensity  $I \propto \langle \hat{a}_i^+ \hat{a}_i \rangle$ . Since the two output photons of the SP-FWM process are highly correlated, the intensity noise correlation function  $G^{(2)}(\tau)$  between  $\mathbf{E}_S$  and  $\mathbf{E}_{aS}$  signal can be calculated by [19]

$$G_{S-aS}^{(2)}(\tau) = \langle (\delta \hat{I}_S(t_S))(\delta \hat{I}_{aS}(t_{aS})) \rangle / \sqrt{\langle (\delta \hat{I}_S(t_S))^2 \rangle \langle (\delta \hat{I}_{aS}(t_{aS}))^2 \rangle} \quad (8)$$

where  $\tau$  is the selected time delay between the Stokes and anti-Stokes signals. Without any injection,  $G_{S-aS}^{(2)}(\tau)$  can be rewritten as

$$G_{aS-S}^{(2)}(\tau) = A / \sqrt{BCDE} \quad (9)$$

where  $A = R_1 \left| \int d\omega_{aS} e^{-i\omega_{aS}\tau} \cosh(\kappa L) \sin h(\kappa L) \right|^2$ ,  $B = R_2 \int d\omega_S \sin h(\kappa L) \sin h(\kappa L)$ ,  $C = R_3 \int d\omega_{aS} \sin h(\kappa L) \sin h(\kappa L)$ ,  $D = R_4 \int d\omega_S \cos h(\kappa L) \cos h(\kappa L)$ ,  $E = R_5 \int d\omega_{aS} \cos h(\kappa L) \cos h(\kappa L)$ ,  $R_1 = |R_S R_{aS} \mathbf{E}_S \mathbf{E}_{aS}|^2$ ,  $R_{2,4} = R_S |\mathbf{E}_S|^2$ ,  $R_{3,5} = R_{aS} |\mathbf{E}_{aS}|^2$  with  $R_{aS/S} = V^{1/3} / [(2\pi)v_{aS/S}]$  and  $\mathbf{E}_{aS/S} = (\hbar\omega_{aS/S}/2\epsilon_0 V)^{1/2}$  (here,  $V$  is the quantization volume and  $v_{aS/S}$  is group velocity). For the parameters in above expressions, only  $A$  is related to  $\tau$ .

We also investigate the squeezing in  $V$  and  $\Lambda$ -type systems, which is governed by [20].

$$Sq = \text{Log}_{10} \left[ \delta^2(\hat{I}_S - \hat{I}_{aS}) / \delta^2(\hat{I}_S + \hat{I}_{aS}) \right] = \text{Log}_{10} \left[ \delta^2(\hat{N}_S - \hat{N}_{aS}) / \delta^2(\hat{N}_S + \hat{N}_{aS}) \right] \quad (10)$$

where  $\delta^2(\hat{N}_S - \hat{N}_{aS})$  and  $\delta^2(\hat{N}_S + \hat{N}_{aS})$  are the mean square deviation of the intensity difference and intensity sums, respectively.

The generated intensity noises correlation and intensity difference squeezing in the SP-FWM process are related to the nonlinear coefficient  $\kappa$ , which can be modified by the dressing effect induced by  $\mathbf{E}_1$  and  $\mathbf{E}_2$  (or  $\mathbf{E}_3$ ). Specially, the dressing effects can be manipulated by the detuning and power of the incident fields. So both correlation and squeezing can be changed via the detuning and power.

### 2.2.3 Coherence time and decay rate of Stokes and anti-Stokes

Besides, we investigate the coherence time of the generated intensity noise correlation. The intensity of Stokes or anti-Stokes signal is related to the respective number of photon and can be expressed by

$$I(t) = N_{S/aS} e^{-\Gamma_{S/aS} t} \quad (11)$$

where  $\Gamma_S/\Gamma_{aS}$  are decay rates whose values are different in  $\Lambda$  and  $V$  type system. In the  $\Lambda$  system,  $\Gamma_{S2} = \Gamma_{13} + \Gamma_{30} + \Gamma_{10}$  and  $\Gamma_{aS2} = \Gamma_{10} + \Gamma_{30} + \Gamma_{10}$ , and for  $V$  level system  $\Gamma_{S1} = \Gamma_{20} + \Gamma_{00} + \Gamma_{20}$  and  $\Gamma_{aS1} = \Gamma_{10} + \Gamma_{00} + \Gamma_{20}$ , in which  $\Gamma_{00} = (2\pi T_1)_0^{-1} + (2\pi T_2^*)_0^{-1}$  is the transverse dephasing rate of the ground state  $|0\rangle$ .

### 3. Results and discussions

#### 3.1 Intensity noise correlation and intensity difference squeezing with changing detuning

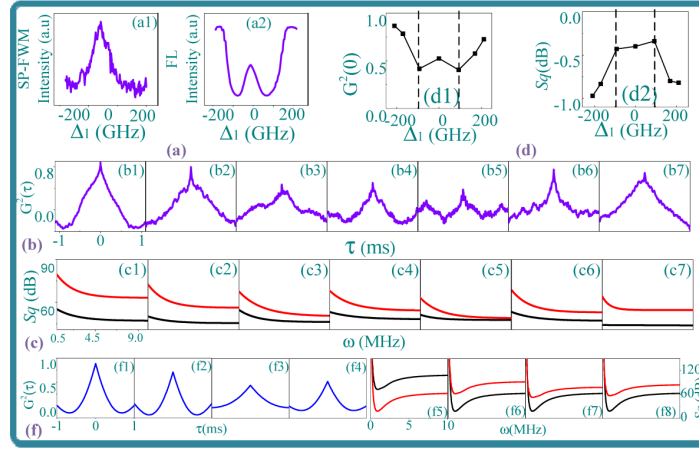


Fig. 2. (a) Spectrum intensity of signals: (a1) Stokes SP-FWM signal, and (a2) fluorescence signal in  $\Lambda$ -type level system; (b1-b7) Intensity Noise correlation functions  $G^{(2)}(\tau)$  of Stokes and anti-Stokes versus delayed time  $\tau$ , with  $\Delta_1$  set to  $-200\text{GHz}$ ,  $-170\text{GHz}$ ,  $-92\text{GHz}$ ,  $0\text{GHz}$ ,  $92\text{GHz}$ ,  $170\text{GHz}$  and  $200\text{GHz}$ , respectively; (c1-c7) Intensity-difference squeezing versus analysis frequency  $\omega$  obtained with the same experimental parameters to (b1-b7), respectively; (d1) Detuning dependence of the correlation value  $G^{(2)}(0)$ , and (d2) Detuning dependence of the intensity-difference squeezing at  $1.5\text{MHz}$ . (f1-f4) The theoretical simulation results of dressed correlation in accordance with (b1-b4) and (f5-f8) theoretical simulated squeezing in accordance with (c1-c4).

We first investigate the intensity noise correlation between the Stoke and anti-Stokes signals in the  $\Lambda$ -type level system. Figure 2(a1) and 2(a2) show the measured Stokes signal and the fourth order fluorescence signal, respectively. These signals are obtained by scanning  $\Delta_1$  from  $-200\text{GHz}$  to  $200\text{GHz}$  and keeping  $\Delta_3 = 0$ . The  $\mathbf{E}_1$  and  $\mathbf{E}_3$  fields have horizontal polarization and their powers keep  $2\text{mW}$ . The fluorescence signal appears a suppression dip with a weak peak at resonance. This phenomenon can be explained by the dressing effect, which will change from single dressing (from  $\mathbf{E}_3$  field) to double dressing (from  $\mathbf{E}_3$  and  $\mathbf{E}_1$  field) when  $\Delta_1$  is changed from  $-200/200\text{GHz}$  to  $0\text{GHz}$ . Since the generated Stokes signal is less sensitive to dressing effect than fluorescence signal, so we cannot observed the double dressing from it [21].

Figures 2(b1-b7) show the intensity noise correlations of Stokes and anti-Stokes versus delayed time  $\tau$  with different detuning  $\Delta_1$ . The square points in Fig. 2(d1) show the dependence of correlation (with  $\tau = 0$ ) on detuning of  $\Delta_1$ . It is found that the correlation values  $G^{(2)}(0)$  become weaker when  $\Delta_1$  is tuned from larger detuning ( $\pm 200\text{GHz}$ ) to near resonance ( $\pm 92\text{GHz}$ ) with the energy level  $|1\rangle$ , there exists a poorest correlation at  $\Delta_1 = -92/92\text{GHz}$ . Then the correlation will slightly increase when  $\Delta_1$  is at resonance ( $0\text{GHz}$ ). According to Eq. (5-8),  $G^{(2)}(0)$  depends on the nonlinear susceptibility  $\chi_{S/aS}^{(3)}$ . This result reflects the induced modulation of nonlinear susceptibility ( $\chi_{S/aS}^{(3)}$ ) by the dressing effect. The  $\chi_{S/aS}^{(3)}$  is function of the density matrix elements  $\rho_{(S/aS)}^{(3)}$ , in which dressing terms  $G_3^2/[\Gamma_{13+i(\Delta_1-\Delta_3)}]$  of  $\mathbf{E}_3$  and  $G_1^2/[\Gamma_{13+i\Delta_1}]$  of  $\mathbf{E}_1$  in Eq. (1-2) will affect  $\chi_{S/aS}^{(3)}$ . When we tune  $\Delta_1$  near the two dressed states, the nonlinear optical susceptibility  $\chi_{S/aS}^{(3)}$  can be enhanced due to the two-photon resonance

[22]. So we can control the intensity-noise correlation by altering  $\Delta_1$ . When  $\Delta_1$  is set to  $-200/200$  GHz, the  $\mathbf{E}_1$  field will be near-resonant to the two dressed states, therefore, the  $\chi_{S/aS}^{(3)}$  can be enhanced. Hence the correlation is the highest at  $-200/200$  GHz. When  $\Delta_1$  is tuned away from the two dressed states, the  $\chi_{S/aS}^{(3)}$  will gradually decrease as shown at points  $-170/170$  GHz and  $-92/92$  GHz. According to the above dressed-state analysis, at  $\Delta_1 = 0$ , the correlation should be the poorest. However, the correlation at  $\Delta_1 = 0$  is higher than that at  $-92/92$  GHz. This is because the dressing from  $\mathbf{E}_1$  field is also active at  $\Delta_1 = 0$ , where the higher correlation is induced by double dressing from  $\mathbf{E}_1$  and  $\mathbf{E}_3$ . These results are also shown through theoretical simulation of dressed correlation function of Eq. (8) in Fig. 2(f1-f4) in accordance with Fig. 2(b1-b4), respectively. The experimental results agree well with the theoretical simulated results.

At the meantime, by substituting the detected intensity data into Eq. (10), we can also obtain the intensity-difference squeezing of Stokes and anti-Stokes signal as shown in Figs. 2(c1-c7), where the intensity-difference squeezing  $\delta^2(\hat{N}_S - \hat{N}_{aS})$  and the total sum of noise spectra  $\delta^2(\hat{N}_S + \hat{N}_{aS})$  versus  $\omega$  are shown by the lower curves and the higher curves, respectively. According to Eq. (5) and (10), the squeezing also depends on  $\chi_{S/aS}^{(3)}$ . Figure 2(d2) gives the degree of squeezing amount at different detuning  $\Delta_1$  when the analysis frequency  $\omega$  is set at 1.5MHz. One can easily see that the intensity-difference squeezing in Fig. 2(c) have the same behavior with that of correlation in Fig. 2(b). Hence, by changing  $\Delta_1$  and then the dressing effect, the degree of intensity-difference squeezing of the output  $\mathbf{E}_S$  and  $\mathbf{E}_{aS}$  fields can also be controlled. Figures 2(f5-f8) show theoretical simulation of squeezing by Eq. (10) corresponding to experimental result of squeezing ((Fig. 2(c1-c4)). The experimental results can be well explained by the theoretical model.

Now we investigate the intensity noise correlation in a V-type level system with the same power and polarization defined for  $\Lambda$ -type level system. The intensities of Stokes signal and fourth order fluorescence signal are shown in Figs. 3(a1) and (a2), respectively, with  $\Delta_1$  scanned ( $-200$  to  $200$  GHz) and  $\Delta_2$  ( $\Delta_2 = 0$ ) fixed. Differentiating from the signal in  $\Lambda$ -type level system (a suppression dip), the fluorescence signal in V-type level shows an emission peak. This indicates the energy levels of V-type system are less sensitive to dressing effect than that in  $\Lambda$ -type system, because the dressing effect between levels of individual ion is stronger than hetero-nuclear-like configuration.

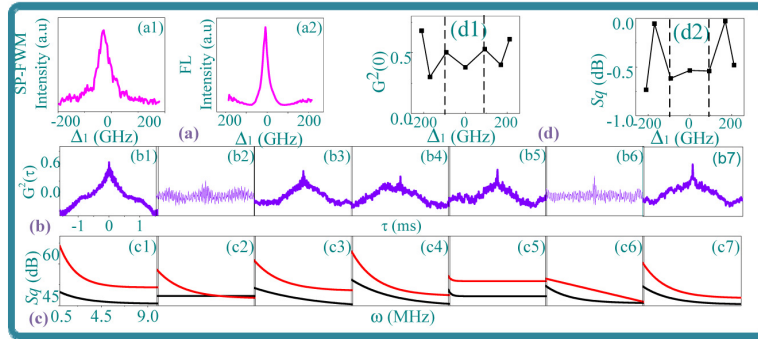


Fig. 3. (a) Spectrum intensity of signals: (a1) Stokes SP-FWM signal and (a2) fluorescence signal in V-type level system; (b1-b7) Intensity Noise correlation function  $G^{(2)}(\tau)$  of Stokes and anti-Stokes versus delayed time  $\tau$ , by setting  $\Delta_1$  to be  $-200$ GHz,  $-170$ GHz,  $-92$ GHz,  $0$ GHz,  $92$ GHz,  $170$ GHz and  $200$  GHz, respectively; (c1-c7) Intensity-difference squeezing versus analysis frequency  $\omega$  in accordance with (b1-b7), respectively; (d1) Detuning dependence of the correlation value  $G^{(2)}(0)$ , and (d2) detuning dependence of the value of  $S_I$  at 1.5 MHz.

Following the same procedure just as in the  $\Lambda$ -type system, the intensity noise correlations between Stokes and anti-Stokes and their intensity difference squeezing are obtained as shown in Figs. 3(b1-b7) and 3(c1-c7), respectively. Figures 3(d1) and 3(d2) show the dependence of correlation function  $G^{(2)}(0)$  at  $\tau=0$  and squeezing at  $\omega=1.5\text{MHz}$  versus  $\Delta_1$ , respectively. In Figs. 3(b1-b7), it is found that the correlation value  $G^{(2)}(0)$  has large value at  $\pm 200\text{GHz}$  and decreases when  $\Delta_1$  is tuned to  $\pm 170\text{GHz}$ . However, it increases with further decrease of  $\Delta_1$ , and then slightly decreases when  $\Delta_1$  is set at resonance. This result also reflects the dressing-induced modulation of  $\chi_{S/aS}^{(3)}$ , but the phenomenon is not exactly the same to the  $\Lambda$ -type system. From Eq. (3-4) we can find a different nested dressing term  $|\Gamma_2|^2/[\Gamma_{20}+i(\Delta_2-\Delta_1)+\Gamma_1]^2/[\Gamma_{01}-i\Delta_1]$  in the V-type system. When  $\Delta_1$  is tuned near the 0GHz, the higher-order nonlinear process becomes strong and interferes with the SP-FWM process. Hence oscillation of the correlation can be observed near the 0GHz. Again, squeezing in Fig. 3(c) has the same behavior as the correlation. Comparing V-type with  $\Lambda$ -type system, besides the oscillation of correlation and squeezing, the maximum value of the correlation and squeezing are obtained in  $\Lambda$ -type system is larger than that in V-type system.

### 3.2 Intensity noise correlation and intensity difference squeezing with changing power

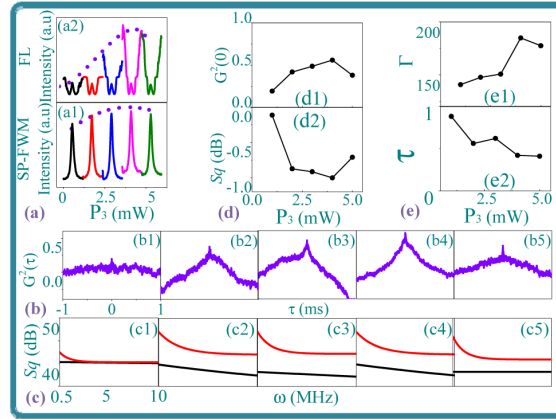


Fig. 4. (a) The measured signals versus  $\Delta_1$  at different  $P_3$  power in  $\Lambda$ -type level system: (a1) Spectrum intensity of Stokes SP-FWM signal, and (a2) intensity of fluorescence. (b1-b5) Intensity noise correlation functions  $G^{(2)}(\tau)$  between Stokes and anti-Stokes signals with fixing  $\Delta_1 = \Delta_3 = 0$  and setting  $P_3$  power from 1, 2, 3, 4 to 5 mW, respectively. (c1-c5) The calculated intensity-difference squeezing with the same experimental parameters in accordance with (b1-b5), respectively. (d1) The power dependence of correlation value  $G^{(2)}(0)$  at  $\tau = 0$ . (d2) The power dependence of intensity-difference squeezing at 1.5 MHz. (e1) Decay rate calculated from  $\Gamma_{S2}$  and  $\Gamma_{aS2}$  in time domain and (e2) Calculated correlation time from (b).

Subsequently, we investigate the power dependence of the correlation and squeezing. Five curves in Fig. 4(a1) show the intensity of output Stokes signal versus  $\Delta_1$  (from  $-200\text{GHz}$  to  $200\text{GHz}$ ) with fixed  $\Delta_3 = 0$  in the  $\Lambda$ -type level system, while the power  $P_3$  are changed from 1mW to 5mW. The signal strength increases with the power  $P_3$  up to 4mW due to the gain effect of  $\mathbf{E}_3$  field, but then decrease at 5 mW due to enhanced dressing effect from  $\mathbf{E}_3$  field. Figure 4(a2) shows the measured fourth-order fluorescence signals versus  $\Delta_1$  in the same way as the Fig. 4(a1). One can see the depth of the suppressed dip is same, but the baseline increases with  $P_3$  at first, and then decreases when  $P_3 = 5\text{mW}$ . The baseline indicated by short-dashed curve is the non-resonant fluorescence, which presents similar changing trend with  $P_3$  from the gain effect to dressing effect.



Figures 4(b1-b5) show the correlation functions  $G^{(2)}(\tau)$  at different powers. The corresponding intensity-difference squeezing is shown in Figs. 4(c1-c5), Figs. 4(d1) and 4(d2) is the correlation dependence of  $G^{(2)}(0)$  and squeezing dependence at 1.5 MHz, respectively. From Figs. 4(b1-b5) we can find the correlation value  $G^{(2)}(0)$  increases first with power  $P_3$  from 1mW to 4mW. But  $G^{(2)}(0)$  tends to decrease when the power reaches  $P_3 = 5$ mW. At low power region,  $\mathbf{E}_3$  field mainly acts as a generation field, nonlinear gain increases with  $G_3 = \mu E_3 / \hbar$ , so the correlation value  $G^{(2)}(0)$  increases. When the power of  $\mathbf{E}_3$  field is strong enough, we should consider dressing effect from  $\mathbf{E}_3$ . According to Eq. (1-2), the density matrix elements will decrease with  $G_3$ , so the correlation decreases. The intensity difference squeezing as shown in Figs. 4(c1-c5) has the same behavior with the correlation.

Figures 4(e1) and 4(e2) show the decay rate and the calculated correlation time of SP-FWM, respectively. Because the decoherence rate  $\Gamma_{S2} = \Gamma_{13} + \Gamma_{30} + \Gamma_{10}$  and  $\Gamma_{aS2} = \Gamma_{10} + \Gamma_{30} + \Gamma_{10}$  is caused by the combination of the dressing effect and induced dipole-dipole interaction (in turn,  $H-H^*$  states and  $D-D$  states, respectively), so one can see that decoherence rate increases with increasing power until the dressing effect is not dominant, then begins to decrease once the dressing effect gets dominant. On the other hand, because the PC-FWM signals are from the coherent processes, so the correlation times are determined by decoherence time (or inversely proportional to decoherence rate) of PC-FWM process, one can see inverse evolution on power between decay rate and the correlation time.

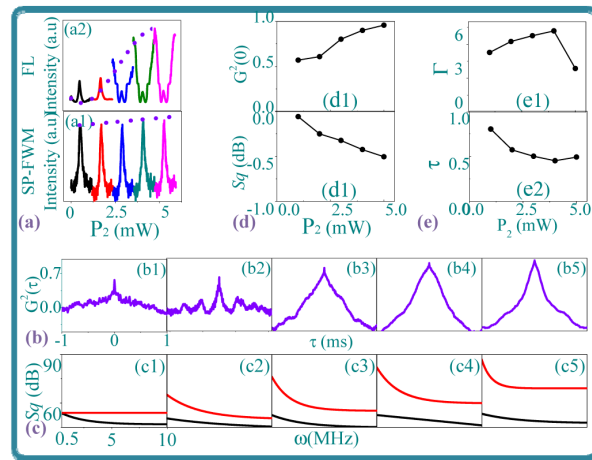


Fig. 5. (a) The measured signals versus  $\Delta_1$  at different  $P_2$  power in V-type level system: (a1) Spectrum intensity of Stokes SP-FWM signal, and (a2) intensity of fluorescence. (b1-b5) Intensity noise correlation between Stokes and anti-Stokes signals with fixing  $\Delta_1 = \Delta_2 = 0$  and setting  $P_2$  power from 1, 2, 3, 4 to 5 mW, respectively. (c1-c5) The calculated intensity-difference squeezing with the same experimental parameters in accordance with (b1-b5), respectively. (d1) The power dependence of correlation with  $\tau = 0$  in accordance with (b). (d2) The power dependence of intensity-difference squeezing at 1.5 MHz. (e1) Decay rate calculated from  $\Gamma_{S2}$  and  $\Gamma_{aS2}$  in time domain and (d2) calculated correlation time from (b).

Figure 5(a1) and (a2) show the intensities of output Stokes signal and fourth-order fluorescence signals at different power  $P_2$  in the V-type level system, respectively. We can see the fourth-order fluorescence signals change from a generation peak to a suppressed dip with  $P_2$  increasing because the dressing effect of  $\mathbf{E}_2$  field enhances. The baseline is the second-order fluorescence from  $|2\rangle$  to  $|0\rangle$ , which is increased with  $P_2$  due to gain effect. At the same time, the SP-FWM signals also become stronger with the increasing of  $P_2$ . The dressing effect on SP-FWM in V-type level system is weaker than that of  $\Lambda$ -type system. Figures 5(b1-b5) give

the correlation functions between Stokes and anti-Stokes signals with power  $P_2$  increasing. Following, the corresponding intensity-difference squeezing at different  $P_2$  are shown in Figs. 5(c1-c5). Figures 5(d1) and 5(d2) show the corresponding correlation value  $G^{(2)}(0)$  and the squeezing amount at 1.5 MHz, respectively. The correlation and squeezing increases with the same fashion as increased power due to increased nonlinear gain. Unlike the  $\Lambda$ -type level system, where correlation and squeezing decreases at high power due to enhanced dressing effect, the V-type system is less sensitive to dressing of  $\mathbf{E}_2$  field. The power dependences of decay rate and correlation time (as shown in Figs. 5(e1) and 5(e2)) in V-type system are as similar as that in  $\Lambda$ -type system.

#### 4. Conclusion

The dressed noise correlation and intensity-difference squeezing based on SP-FWM process in  $\text{Pr}^{3+}:\text{Y}_2\text{SiO}_5$  crystals have been observed experimentally and theoretically both in  $\Lambda$ -type and V-type systems. We observed that the degree of correlation and squeezing of the Stokes and anti-Stokes signals can be controlled by detuning and power. These results are attributed to dressing-induced modulation of nonlinear susceptibility. It is also observed difference of correlation behaviors between  $\Lambda$ -type and V-type systems due to different dressing effects on levels of individual ion and hetero-nuclear-like configuration. Further, the noise correlation and the intensity-difference squeezing are dependent on power of optical field. So we can control them by power easily. It is clearly seen that the dressed results of squeezing have the same behavior with the correlation. In addition, we find the dressing effect can also be observed through the fourth-order fluorescence signals. We also studied the power dependences of correlation time and decoherence rate. Results predict that the decoherence rate increases with increasing power until the dressing effect is not dominant. Once the dressing effect gets dominant, the decoherence rate starts to decrease. Such controllable intensity correlation and squeezing of SP-FWM process can be used to fabricate entangled light sources in quantum communication.

#### Acknowledgments

This work was supported by the National Basic Research Program of China (2012CB921804), the National Natural Science Foundation of China (11474228, 61205112), and Key Scientific and Technological Innovation Team of Shaanxi Province (2014KCT-10).